Scientific Research Publishing

International Journal of Geosciences, 2024, 15, 1064-1086
https://www.scirp.org/journal/ijg
ISSN Online: 2156-8367
ISSN Print: 2156-8359

Flood Risk Modelling Using the HFPA (Hierarchical Fuzzy Process Analysis) Method: Example of the City of Thies, Senegal

Seybatou Dieye[1], Mapathé Ndiaye[2], Diogoye Diouf[3], Makhaly Ba[2]

[1]Doctoral School, University Iba Der THIAM of Thies, Thies, Senegal
[2]University Iba Der THIAM of Thies, Thies, Senegal
[3]Iba Der THIAM University, Thies, Senegal
Email: seybatou.dieye@univ-thies.sn

How to cite this paper: Dieye, S., Ndiaye, M., Diouf, D. and Ba, M. (2024) Flood Risk Modelling Using the HFPA (Hierarchical Fuzzy Process Analysis) Method: Example of the City of Thies, Senegal. *International Journal of Geosciences*, **15**, 1064-1086.
https://doi.org/10.4236/ijg.2024.1512056

Received: November 14, 2024
Accepted: December 23, 2024
Published: December 26, 2024

Abstract

Based on the perception of flood risk factors derived from the lessons learned by the main stakeholders, namely the members of the National Emergency Response Plan (ORSEC) and the people affected by floods in the study area (Thies, Senegal), this work consists of modelling the flood risk using Hierarchical Process Analysis (HPA). This modelling made it possible to determine the coherence index (CI) and the coherence ratio, which were evaluated respectively at 0.27% and 5% according to the perception of the members of the ORSEC Plan, and at 0.28% and 5% according to the perception of the disaster victims. These results show that the working approach is coherent and acceptable. We then carried out Hierarchical Fuzzy Process Analysis (HFPA), an extension of HFPA, which seeks to minimize the margins of error. FPHA uses fuzzification of perception contributions, interference rules and defuzzification to determine the Net Flood Risk Index (NFRI). Integrated with ArcGIS software, the NFRI is used to generate flood risk maps that reveal a high risk of vulnerability of the main outlets occupied by human settlements.

Keywords

Flood, Hazard, Vulnerability, Factor, Risk, Coherence Index, Coherence Ratio, Hierarchical Analysis of Fuzzy Processes, Thies

1. Introduction

Floods are one of the most destructive disasters in the world, with considerable economic and social consequences and social damage that no other natural phe-

nomenon in the world causes [1]-[3]. They are also the main cause of natural disasters in the world [4] and are the leading cause of natural disasters, claiming around 20,000 victims a year [5]. The African continent also suffers the effects of flooding. According to the United Nations Organization for the Coordination of Humanitarian Affairs, floods have caused 200 deaths and affected 770,000 people in the West African sub-region [6] [7]. Some researchers point out that between 2000 and 2018, there were 698 flood-related disasters in Africa, killing more than 14,250 people, affecting 45 million people and causing 6.8 million dollars in economic losses [8] [9].

In Senegal, the causes of flooding are partly linked to unsuitable urban planning, high population pressure and poorly controlled urbanization, particularly in non aedificandi zones. In the study area, the partial declassification of classified forests (Thies and Pout), uncontrolled land use, particularly in flood-prone areas, violent run-off and the return of exceptional rainfall are often the causes of flooding.

The aim of this work is to contribute to the modelling of fuzzy spaces, uncertainties and imprecisions in flood risk, taking into account vulnerability to physical and human factors. More specifically, we intend to model flood risk by developing a modified version of Hierarchical Process Analysis—HPA [10]. Despite the popularity of AHP, this method is sometimes criticized for its inability to properly manage the uncertainties and imprecisions inherent in converting linguistic variables into quantitative variables [11] [12].

Linguistic variables are qualitative data derived from lessons learned by flood management stakeholders. The concept of linguistic variables is used to model the state of the system, which is imprecise and uncertain [13]. We use the fuzzification, fuzzy inference and defuzzification processes of hierarchical fuzzy process analysis (HFPA) to enable decision-makers to make the right decision while minimising the margins of imprecision. The aim will therefore be to study the possibilities offered by matrix calculation processes, by comparing pairs of factors, in order to normalize scores derived from the judgements of ORSEC plan members and people affected by flooding, with a view to proposing risk models, identifying net flood risk indices, mapping the flood hazard and determining the physical and human damage.

2. Location of the Study Area

The study area is located 70 km from Dakar, the capital of Senegal, between parallels 14˚45'00" and 14˚51'00" north latitude and meridians 16˚52'00" and 17˚01'00" west longitude (**Figure 1**).

The study area covers 88.24 km^2, or 1.34% of the Thies region. The study area is between a large basin to the north with a surface area of 65.58 km^2, with a total length of the hydrographic network of 58.517 km, giving a drainage density of 0.89 km^{-1}, a medium basin to the south with a surface area of 15.71 km^2 with a total length of the hydrographic network of 11.645 km, giving a drainage density

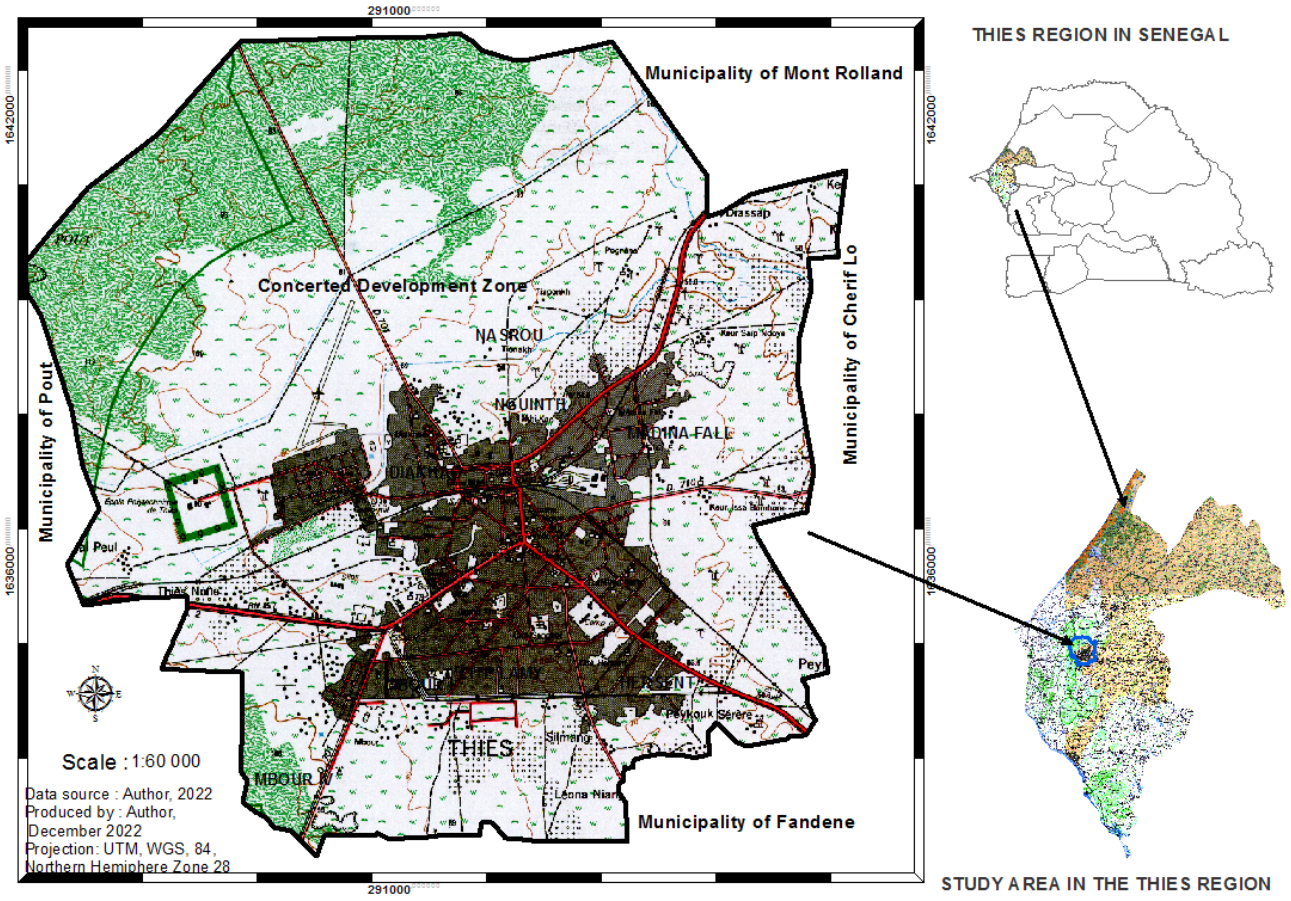

Figure 1. Location of the study area in the Thies region (Data source: ANAT, 2020).

of 0.74 km^{-1}, and a small basin to the east with an area of 690 km^2 and a total length of the hydrographic network of 23.35 km, giving a drainage density of 0.34 km^{-1}.

3. Choice of Comparison Factors

To carry out this work, we identified and selected two flood risk factors: active factors and passive factors. The passive or intrinsic factors that we have selected concern the physical environment (slopes, permeability, porosity and granularity of the soil), the natural environment (plant cover, forest and hydrography), the various networks (density of the hydrographic network, roads and railways, sewage and rainwater drainage network), and human action (land use and implementation of development policies (household waste and buildings). The choice is justified by the physical configuration of the environment, its extent, and the impact of human activity. The active factors are linked to rainfall in terms of intensity, frequency and extent. Our work shows that the Thies region is crossed by six isohyets divided into several classes.

The study area, which lies between the 550 mm and 600 mm rainfall isohyets (Figure 2), has no rivers or lakes. The spatial homogeneity of rainfall, characterised by the existence of an isohyet, led to its omission in the pair-wise comparison

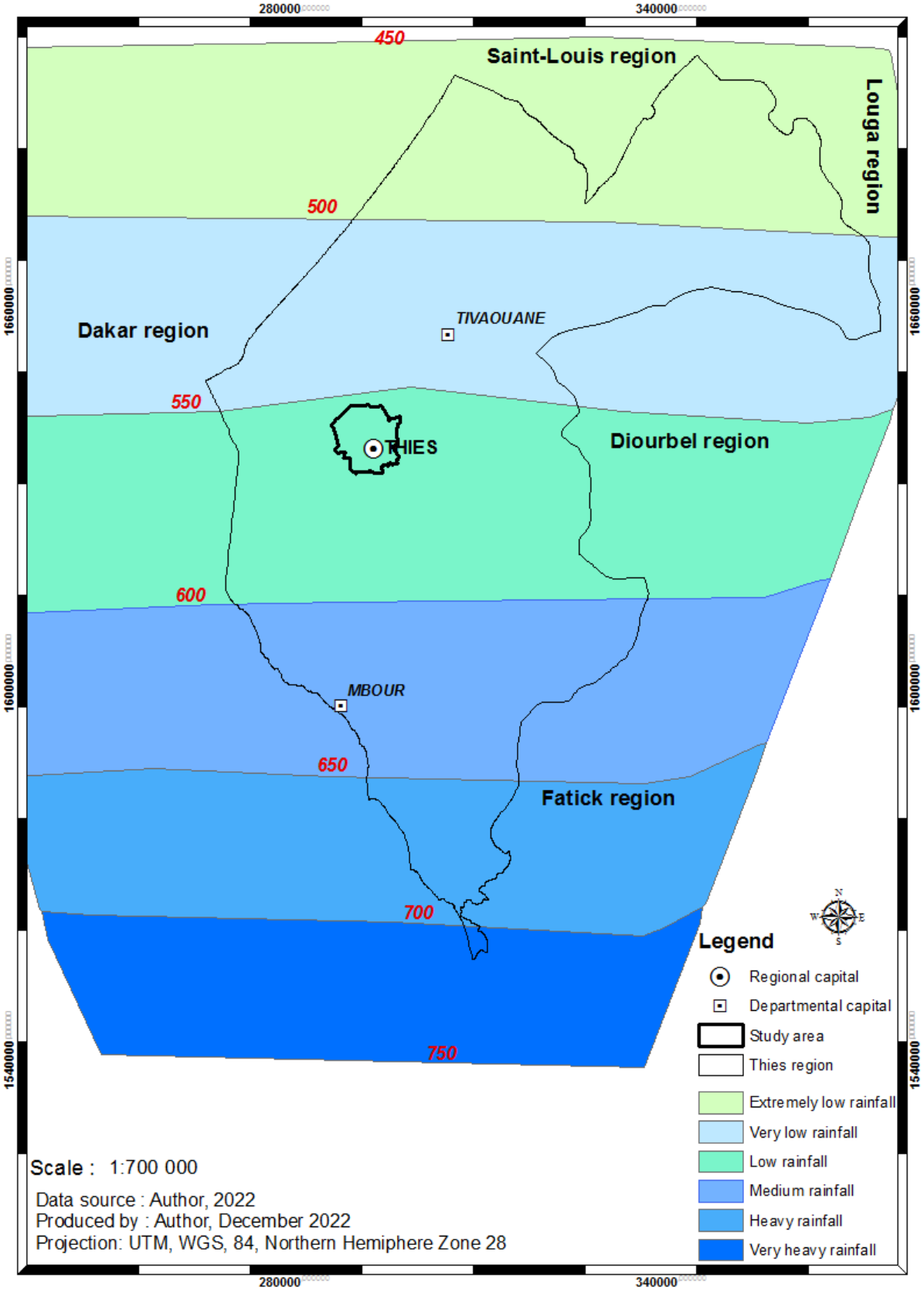

Figure 2. Spatial distribution of isohyets in the Thies region (Data source: ANACIM, Database, 2018).

analysis of flood risk, as well as runoff and flood factors, although in other similar situations they could play a fundamental role. We have therefore omitted rainfall (frequency, duration and intensity), flooding and run-off in the choice of flood risk factors and retained the intrinsic factors.

4. Materials and Methods

4.1. Materials

We then identified the target groups concerned by the problem of flooding in the study area, *i.e.* the members of the Emergency and Organization Service (ORSEC) in charge of flood management and the people affected by flooding. This approach made it possible to collect data on the perception of flood factors by the target groups. To do this, we collected data on soil permeability using the Lefranc test. Darcy's law was used to calculate the soil permeability coefficient (k) according to the following relationship:

$$kSi = Q \tag{1}$$

Q : flow rate in m/s

i : hydraulic gradient in m/m

S : Infiltration surface, corresponding to all surfaces in contact with water (in $mm)^2$

k : Permeability m/s

To produce the soil permeability map, we classified the soil according to Table 1:

Table 1. Classification of the permeability coefficient.

Permeability coefficient k (m/s)	Interpretation
$1.692 \times 10^{-7} < k < 1.01 \times 10^{-6}$	Very watertight
$1.01 \times 10^{-6} < k < 8 \times 10^{-6}$	Low permeability
$8 \times 10^{-6} < k < 10 \times 10^{-6}$	Moderately permeable
$10 \times 10^{-6} < k < 2 \times 10^{-5}$	Permeable
$2 \times 10^{-5} < k < 5 \times 10^{-5}$	Very permeable

This classification was used to draw up the soil permeability map, which will be used as input data for mapping susceptibility to flood risk and for determining the risk susceptibility index.

Figure 3 shows that the soils with low permeability are located in the outflow zones occupied by anarchic populations. Figure 3 will be used as input data for the hierarchical analysis of fuzzy processes.

We also collected "SRTM Plus" data (ASTER, 2013) to produce the digital terrain model.

Figure 4 shows that the study area lies in a basin at the top of which, further to the east, is a ridge covering an area of 140 hectares and with a perimeter of 6,976 meters. This ridge is 124 meters high.

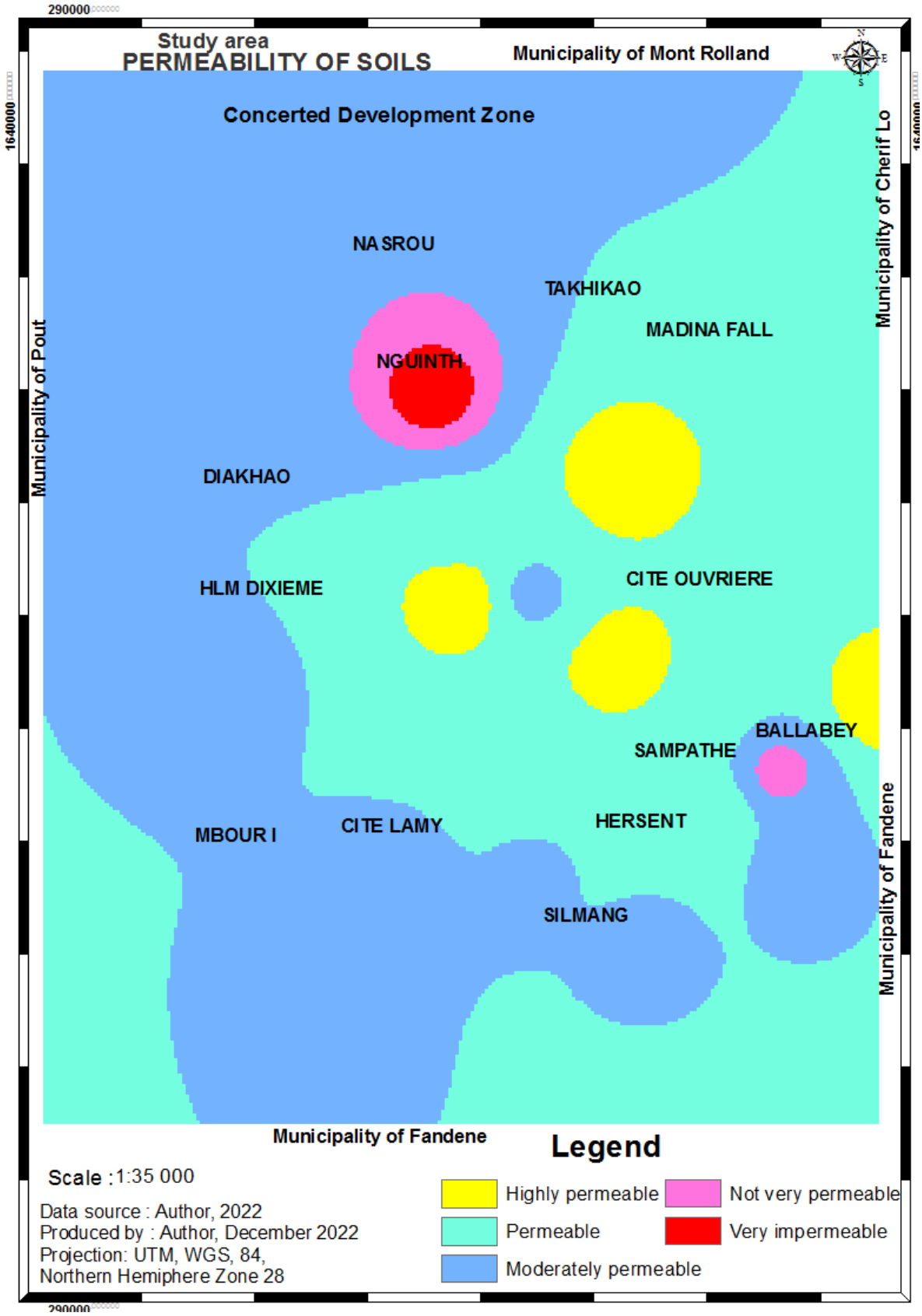

Figure 3. Permeability map.

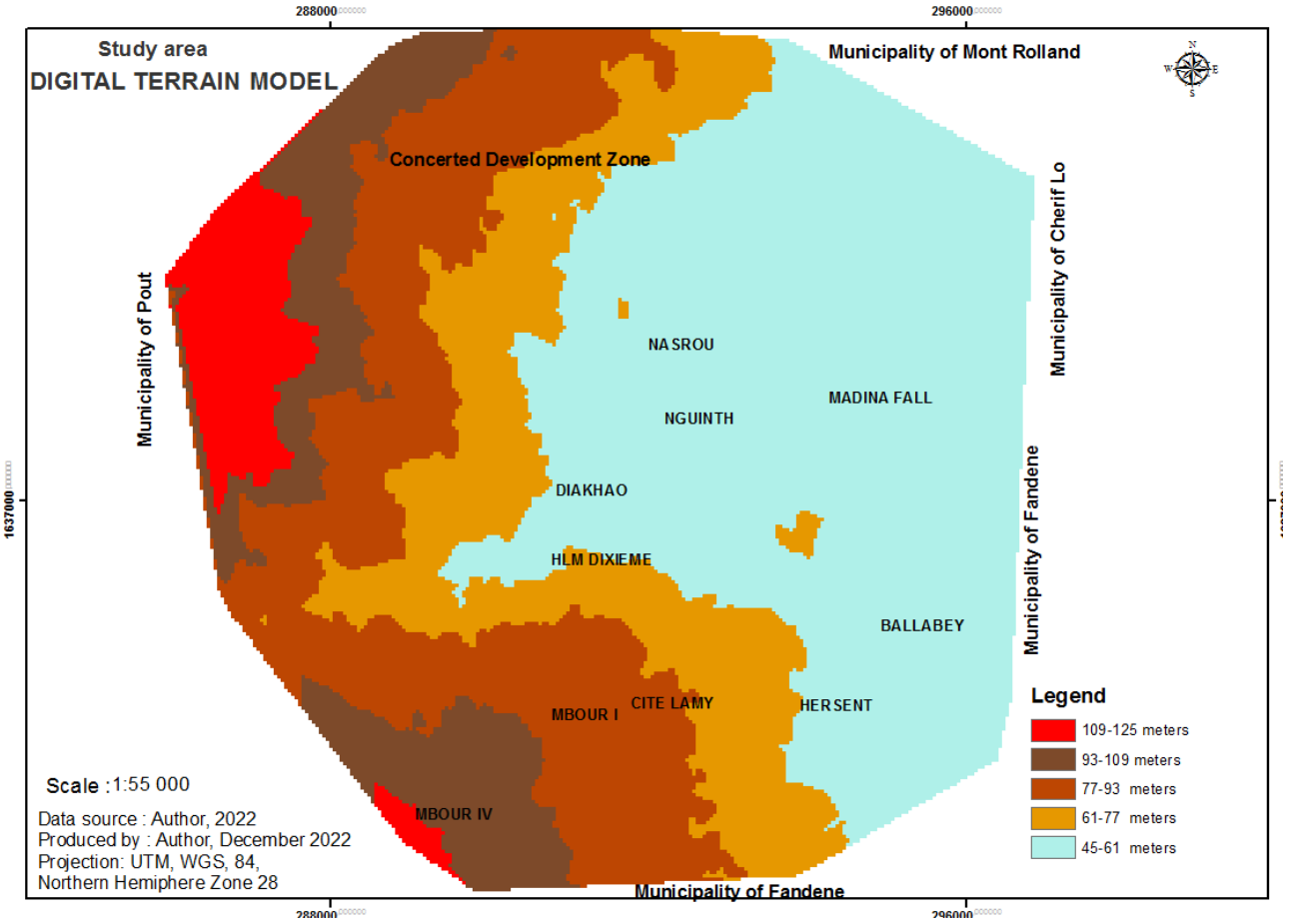

Figure 4. Digital terrain model.

Below this ridge, between 46 and 89 meters above sea level, lies the administrative centre, the primary, tertiary and quaternary sectors, and the defence and security forces.

Figure 4 will be used as an input to the hierarchical analysis of fuzzy processes. To determine the Normalized Difference Vegetation Index (NDVI), we used remote sensing techniques to calculate plant biomass and identify flooded areas and soil typology. We also used Landsat 8 Oli images to determine the NDVI. The ArcGIS Raster Calculator tool was used to apply the formula for Equation (2) of the Normalized Difference Vegetation Index (NDVI), which was used to produce the forest cover map.

$$\mathrm{NDVI} = \frac{\mathrm{NIR} - \mathrm{R}}{\mathrm{NIR} + \mathrm{R}} \tag{2}$$

We also classified the vegetation cover data into five categories with an average amplitude of 7476 pixels. These classes are noted from 1 to 5 and are presented as follows:

- zone of tree vegetation (comprising 7476 pixels),
- zone of semi-wooded vegetation (comprising 16886 pixels),
- zone of medium-tree vegetation (comprising 24549 pixels),

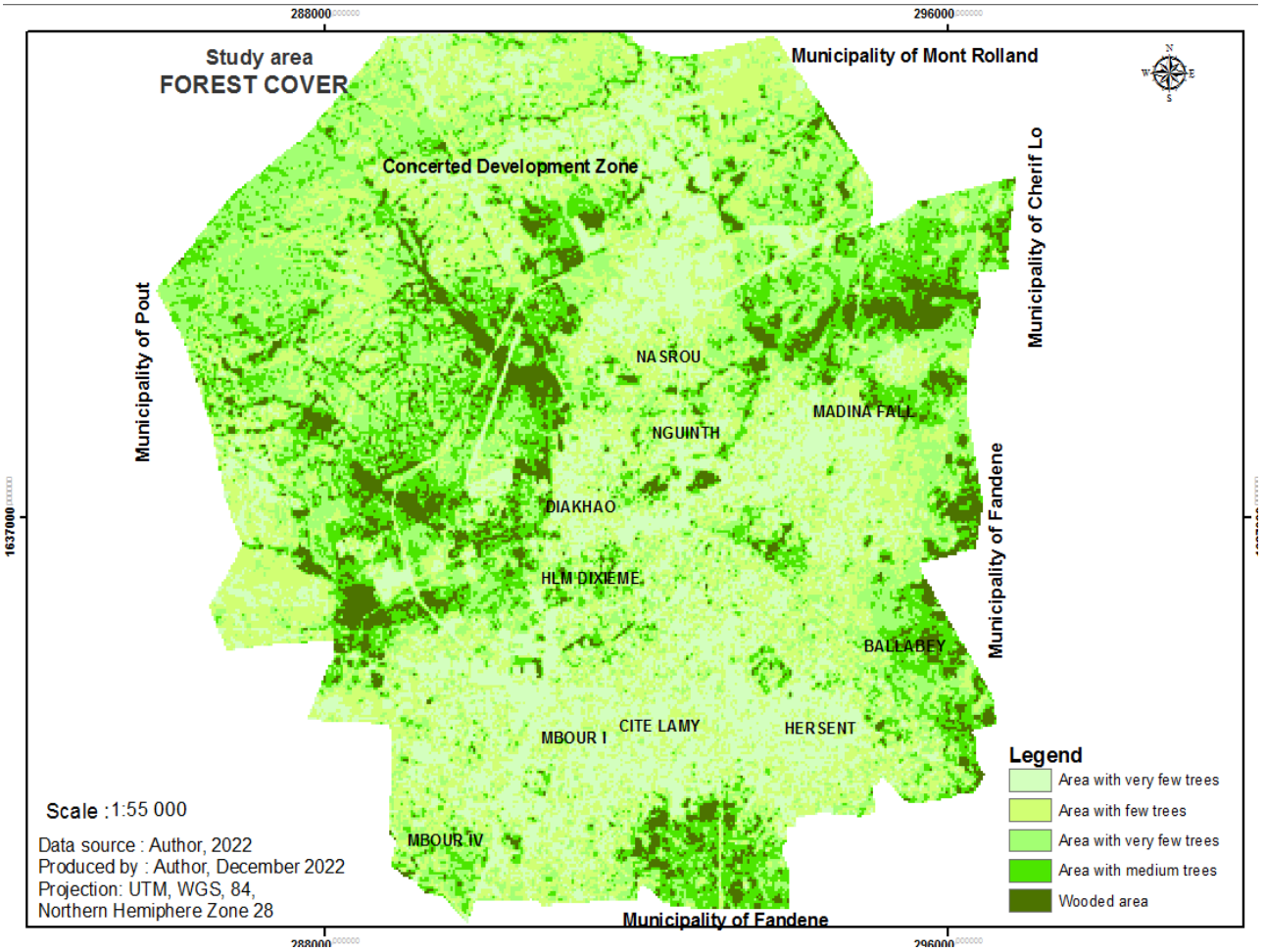

Figure 5. Forest cover in the study area.

- zone of sparse vegetation (comprising 28973 pixels) and,
- zone of very sparse vegetation (comprising 20155 pixels).

Figure 5 will be used as input to the hierarchical fuzzy process analysis. We also used a handheld GPS receiver to survey refuse dumps in order to them.

We have classified the household waste dumps (Figure 6(a)) according to surface area into small, medium and large dumps, rated 1, 3 and 5 respectively. These scores will be used in the modelling.

Figure 6(b) shows the miscellaneous network made up of a set of linear features relating to hydrography, railways, roads and stormwater drainage channels. Data on railways and roads was collected from the land registry. Data on stormwater drainage channels was collected using GPS. Data on the hydrographic network was obtained using remote sensing. After correcting and processing the Aster imagery, we produced maps of the drainage network. The steps involved in determining the hydrographic network.

By superimposing the land parcel data on the soil permeability data layer, we were able to obtain a composite layer covering the potentially flood-prone parts of the study area.

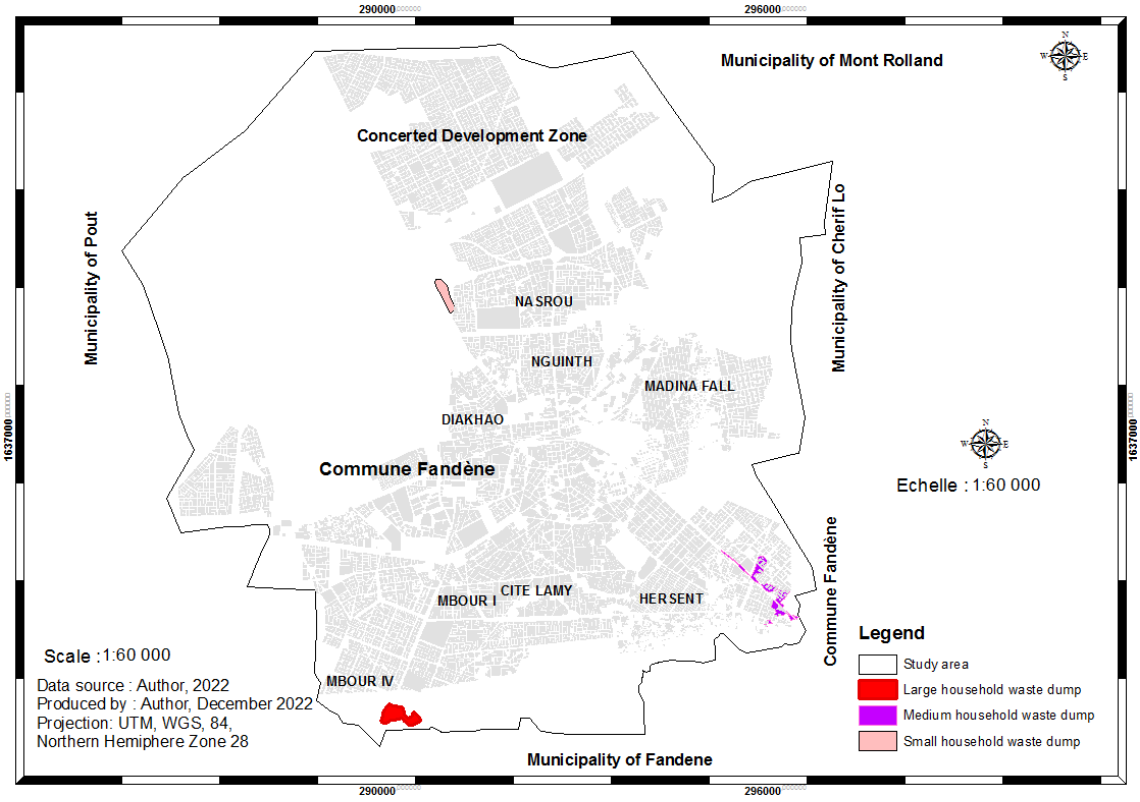

(a)

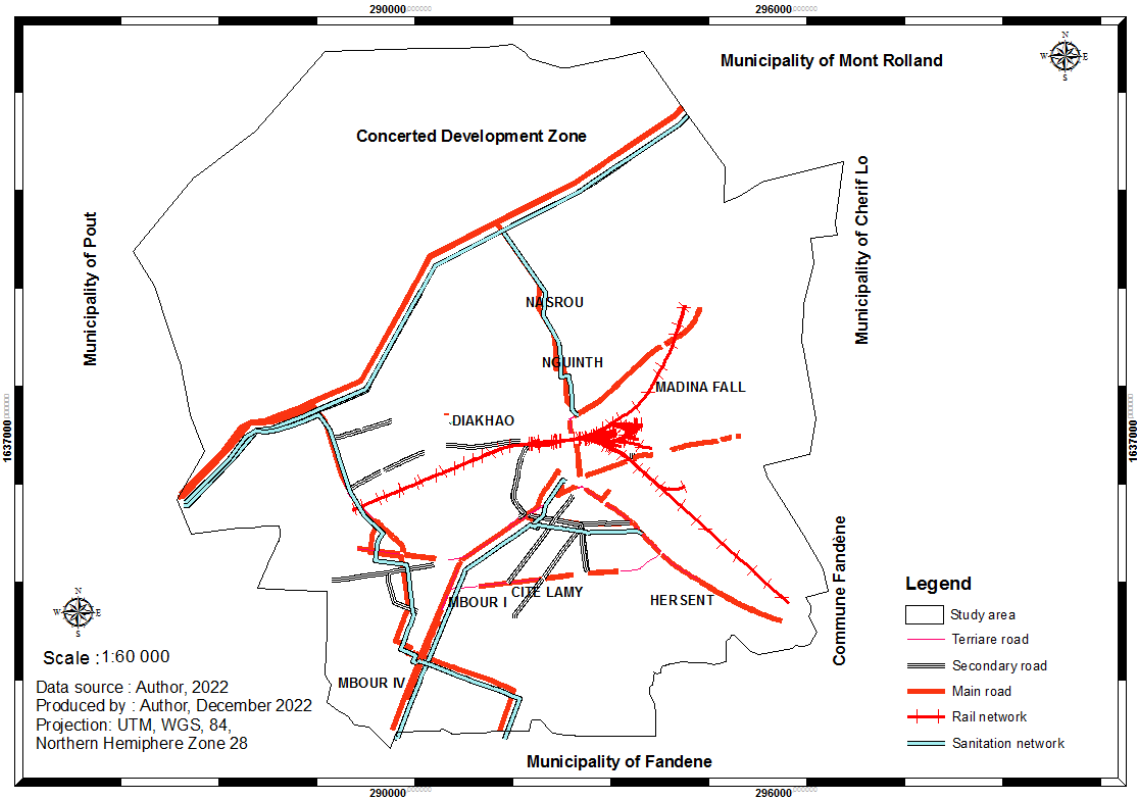

(b)

Figure 6. (a) Map of household waste dumps; (b) map of networks.

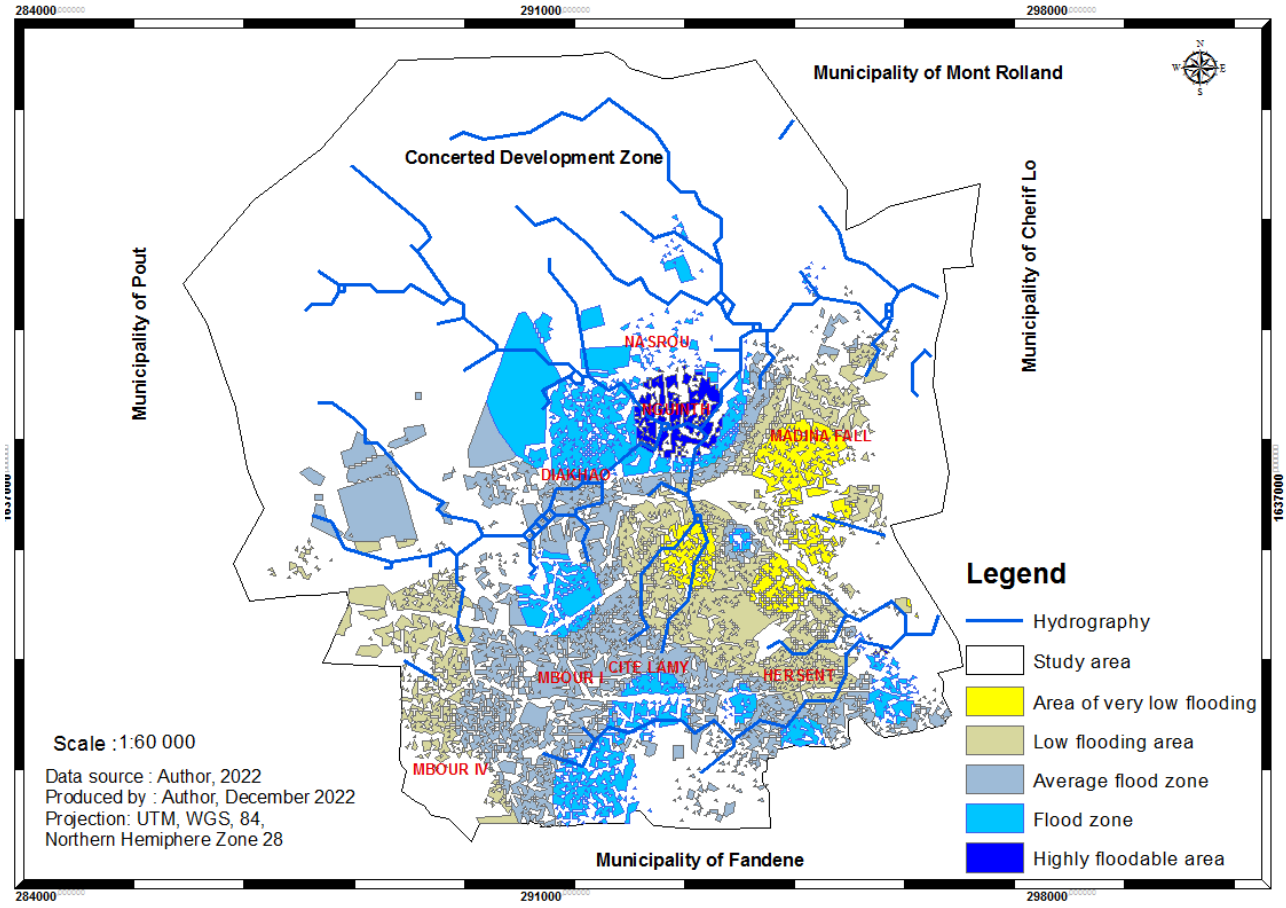

Figure 7. Flood zone map.

Potentially flood-prone areas (Figure 7) have been classified into five categories as follows:

- the very low flooding zone covering an area of 195 ha;
- the low-flood zone covering an area of 632 ha;
- the medium flood zone covering 888 ha;
- The flood zone covers an area of 566 ha;
- the highly floodable zone covering an area of 72 ha.

These data layers are rasterised, classified, declassified and weighted from 1 to 5 according to their influence on the occurrence of floods.

We used three types of software for processing, interpreting and analysing the data: Sphinx Primo version 4.5 for editing the questionnaires, IBM SPSS for processing and analysing the perception data from the pair-wise comparison of factors, and ArcGIS version 10.5 for producing the flood hazard map and determining the physical damage.

To collect data on the perception of the factors, we administered a questionnaire to fifty (50) members of the ORSEC plan (78% from the public service, 8% from the private sector, 6% from local authorities, 6% from civil society and 2% from the Regional Development Agency (RDA)) and to people affected by

the floods. We also administered a questionnaire to the people to be surveyed, and applied a sampling rate of 11%. To do this, we made a selection by superimposing the data from the two soil types with the 6404 plots affected by the effect of run-off. Using the intersection tool, we found 2580 plots, *i.e.* 40% of the total number, to which we applied a sampling rate of 11%, giving us a representative sample of 288 people to survey. This sample was made up of notables (55%), members of women's groups (11%), religious guides (11%), neighborhood delegates (7%), members of community-based organizations (6%), grassroots community organizations (6%) and other categories (4%).

4.2. Method

Hierarchical Fuzzy Process Analysis (HFPA) is the method used in this study. It is based on hierarchical process analysis (HPA), which is a multi-criteria analytical approach to decision support developed by Saaty and before its implementation [14] [15]. The AHP method is used in many fields, including multi-criteria decision making [16] [17]. It is based on complex calculations using matrix algebra [16] [18]. The AHP method reduces the complexity of a decision problem to a sequence of pairwise comparisons, which are synthesised into a ratio matrix that provides a clear rationale for ordering the more and less desirable decision alternatives [19].

Consequently, the AHP is a fundamental step in the implementation of the AHFP method. This is why we go through the conceptualisation of the AHP, the matrix comparison by pair of factors (CMPF) which concerns the linguistic variables, the calculation of the coherences and the validation of the approach. The linguistic variables are qualitative data derived from the lessons learned by flood management stakeholders and relate to: slopes (relief), soil type (permeability), vegetation cover, the various networks (roads, railways, waterways, drainage channels), household waste and buildings (Table 2 and Table 3).

Table 2. Pair-wise comparison matrix of members' perceptions of the ORSEC plan for 2022.

Factors	P	TSP	CV	RD	OM	B
P	1.00	4.32	4.24	4.92	4.60	5.32
TSP	0.23	1.00	3.92	4.32	4.80	5.08
CV	0.24	0.26	1.00	4.00	4.68	5.08
RD	0.20	0.23	0.25	1.00	4.84	5.24
OM	0.22	0.21	0.21	0.21	1.00	5.52
B	0.19	0.20	0.20	0.19	0.18	1.00
SOMME	2.08	6.21	9.82	14.64	20.10	27.24

P: Slope; TSP: Soil type (permeability); CV: Plant cover; RD: Miscellaneous networks; OM: Household waste; B: Buildings.

Table 3. Pair-wise comparison matrix of the perception of people affected by flooding.

Factors	P	TSP	CV	RD	OM	B
P	1.00	4.77	3.82	5.45	4.96	5.02
TSP	0.21	1.00	3.48	4.81	4.69	4.72
CV	0.26	0.29	1.00	4.38	4.37	4.52
RD	0.18	0.21	0.23	1.00	4.95	4.85
OM	0.20	0.21	0.23	0.20	1.00	5.05
B	0.20	0.21	0.22	0.21	0.20	1.00
SOMME	2.06	6.69	8.98	16.05	20.17	25.16

The values of these matrices are obtained by transforming the judgements into numerical values according to the Saaty scale, while respecting the principle of reciprocity [18]: each occurrence of a factor (F_{ij}) in Table 4 is interpreted in both rows and columns.

Table 4. Interpretation of factors—Scale proposed by [20].

Language variable (A and B)	Quantitative variable	Comments/interpretations
Equal importance	1	The two factors A and B are of equal importance
Medium importance	3	Factor A is moderately more important than factor B.
Medium reverse	1/3	Factor B is moderately more important than factor A
High importance	5	Factor A is much more important than factor B
Inverse high importance	1/5	Factor B is much more important than factor A
Very important	7	Factor A is much more important than factor B
Inverse very high importance	1/7	Factor B is much more important than factor A
Intermediate importance	2, 4 and 6	Values associated with intermediate judgements

Using the $\hat{\lambda}_{\max}$ value, the AHP method is used to determine the coherence index.

$$\mathrm{IC} = \frac{\hat{\lambda}_{\max} - n}{n-1} \tag{3}$$

IC of the members of the ORSEC Plan is 0.27 and is equal to 0.28 for people by flooding.

The consistency ratio is the ratio of the consistency index (CI) to the sum of the factors [16] [21]. The consistency ratio (CR) is used to indicate the probability that the judgements in the matrix were randomly generated [22] [23]. Its comparison with Saaty's random Table 5 (TAS) is used to assess the degree of acceptability of the matrix [16].

$$\mathrm{RC} = \frac{\mathrm{IC}}{n} = 5\% \tag{4}$$

We then carry out a comparative analysis of the coherence ratio and the Saaty table. The consistency ratio should be compared with the values shown in Table

5, which relates to the number of factors and the value of the random indices (AI) developed by [10]. It is used to assess the consistency of the approach.

Table 5. Values of random indices (IA) [16].

N	1	2	3	4	5	6	7	8	9	10	11
IA	0.00	0.00	0.58	0.90	1.12	1.24	1.32	1.41	1.45	1.49	1.51

Indeed, according to authors [9] [24] [25], if the consistency ratio RC is greater than or equal to (≥) 10%, this shows that the approach is acceptable. Consequently, we found a CI of 0.27 and an OR of 5%. We assume that the data collected from the players followed an acceptable and consistent pairwise comparison approach.

After validating the consistency approach of the hierarchical process analysis, we proceed with the design and implementation of the Hierarchical Fuzzy Process Analysis (HFPA). Developing an AHPF model means first validating the AHP model, hence the existence of a hyphen between the models. This means that it first integrates the AHP conceptual data model, then validates the consistency of the comparison by pairs of factors and finally approves the approach.

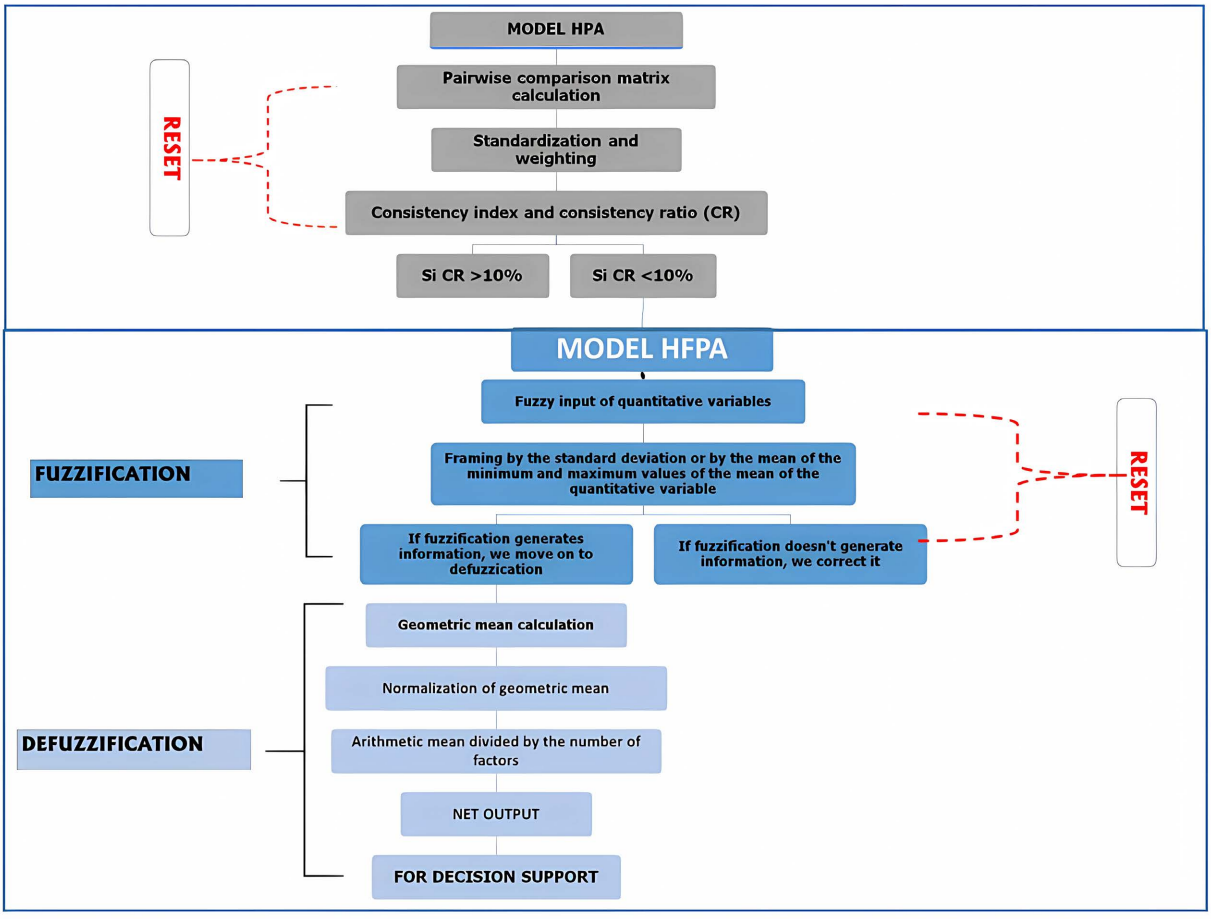

Figure 8. AHPF conceptual model.

This model (Figure 8) shows that the AHPF is based on fuzzy logic, a discipline used in the exact sciences to take account of uncertainty and imprecision [26]. The important aspects of the fuzzy conceptual data model are the membership function, the transformation of linguistic variables into qualitative and quantitative data, and their framing by close values through the processes of fuzzification, inference engines and defuzzification.

In implementing AHPF, we follow four (4) steps with seven (7) techniques. In step 1, we design the fuzzy logic conceptual data model, which is an extension of the AHP model (Figure 8).

In step 2, we carry out fuzzification, which aims to determine the degree of membership of a fuzzy input via membership functions (e.g. triangular, Gaussian, trapezoidal) towards a clear and precise output for decision support [27]. To this end, we fuzzify stakeholder perceptions by pairs of factors. Step 2 consists of four (4) techniques. Technique 1 consists of framing the arithmetic means by the close values as defined by [20].

Table 6. Fuzzification matrix by pair of factors for data derived from the perception of ORSEC Plan members for the year 2022 in the case of the model.

Factors	P			TSP			CV			RD			OM			Be		
P	**1**	**1**	**3**	2	4.32	6	3	4.24	6	3	4.92	6	3	4.6	6	3	5.32	7
TSP	0.17	0.23	0.5	**1**	**1**	**3**	3	3.92	5	2	4.32	6	2	4.8	6	3	5.08	7
CV	0.17	0.24	0.33	0.2	0.26	0.33	**1**	**1**	**3**	2	4	6	2	4.68	6	3	5.08	7
RD	0.17	0.2	0.33	0.17	0.23	0.5	0.17	0.25	0.50	**1**	**1**	**3**	2	4.84	6	3	5.24	7
OM	0.17	0.22	0.33	0.17	0.21	0.5	0.17	0.21	0.50	0.17	0.21	0.50	**1**	**1**	**3**	3	5.52	7
B	0.14	0.19	0.33	0.14	0.2	0.33	0.14	0.20	0.33	0.14	0.19	0.33	0.14	0.18	0.33	**1**	**1**	**3**

In implementing this technique, we apply the framing of each occurrence (Table 6) by the values close to it. For example, the occurrence [PCV] which corresponds to the value of 4.24 is framed by 3 and 6, so we get the matrix [3 4,24 6]. When using technique 2, we use matrix multiplication. For example, as part of the fuzzification by pairs of factors of the data from the perception of the members of the ORSEC Plan (Table 7), the PP matrix [1 1 3] is multiplied by the following matrices: PTSP [2 4.32 6]; P-CV [3 4.24 6]; PRD [3 4.92 6]; P-OM [3 4.6 6]; P-B [3 5.32 7]. We obtain the matrix [162.00 2205.38 27216.00] (Table 8). We also carried out fuzzification (technique 2) by pairs of factors of the data derived from the perception of people affected by flooding for the year 2022 (Table 8). The PP matrix [1 1 3] is multiplied by the following matrices: P-TSP [5 4.77 5]; P-CV [1 3.87 5]; P-RD [3 5.45 7]; P-OM [5 4.96 7]; P-B [3 5.02 7] and we obtain the matrix [225.00 2472.66 36015.00] (Table 9). The fuzzification operation allows us to move from the real domain to the fuzzy domain and consists of determining the degree of membership of a value [28].

If no information is obtained using technique 2, the fuzzification process (technique 1) must be corrected. This correction constitutes technique 3. If the appli-

cation of technique 2 generates information, we proceed with technique 4, in which we calculate the normalisation of the pairwise comparison matrices using the equations below:

$$\beta_{\text{facteur}} = \text{PP} * \text{PPTSP} * \text{PPCV} * \text{PPRD} * \text{PPOM} * \text{PPB} \quad (5)$$

$$\alpha_{\text{facteur}} = \sqrt[n]{\text{PP} * \text{PPTSP} * \text{PPCV} * \text{PPRD} * \text{PPOM} * \text{PPB}} \quad (6)$$

Technique 4, which consists of calculating the geometric mean (Equations (5) and (6)), is also used to produce Table 8 and Table 9.

Table 7. Defuzzification matrix by pair of factors for data derived from the perception of people affected by flooding for the year 2022 in the case of the model.

Factors	P			TSP			CV			RD			OM			B_e		
P	**1**	**1**	**3**	2	4.32	6	3	4.24	6	3	4.92	6	3	4.6	6	3	5.32	7
TSP	0.17	0.23	0.5	**1**	**1**	**3**	3	3.92	5	2	4.32	6	2	4.8	6	3	5.08	7
CV	0.17	0.24	0.33	0.2	0.26	0.33	**1**	**1**	**3**	2	4	6	2	4.68	6	3	5.08	7
RD	0.17	0.2	0.33	0.17	0.23	0.5	0.17	0.25	0.5	**1**	**1**	**3**	2	4.84	6	3	5.24	7
OM	0.17	0.22	0.33	0.17	0.21	0.5	0.17	0.21	0.5	0.17	0.21	0.50	**1**	**1**	**3**	3	5.52	7
B	0.14	0.19	0.33	0.14	0.2	0.33	0.14	0.20	0.33	0.14	0.19	0.33	0.14	0.18	0.33	**1**	**1**	**3**

Table 8. Standardised defuzzification matrix of perceptions for the year 2022 of ORSEC Plan members (AHPF 2022 model).

Factors	β_{facteur}	α_{facteur}	β_{facteur}	α_{facteur}	β_{facteur}	α_{facteur}
P	162.00	2.33	2205.38	3.61	27216.00	5.48
TSP	18.00	1.62	95.59	2.14	630.00	2.93
CV	1.33	1.05	5.72	1.34	25.20	1.71
RD	0.50	0.89	0.30	0.82	0.58	0.91
OM	0.13	0.71	0.01	0.47	0.02	0.50
B	0.00	0.40	0.00	0.25	0.00	0.24
Total = δ		7.00 = 1sδ		8.62 = 2sδ		11.78 = 3sδ

Table 9. Standardised defuzzification matrix of perceptions for the year 2022 of people affected by flooding (AHPF 2022 model)

Factors	β_{facteur}	α_{facteur}	β_{facteur}	α_{facteur}	β_{facteur}	α_{facteur}
P	225.00	2.47	2472.66	3.68	36015.00	5.75
TSP	25.00	1.71	77.68	2.07	735.00	3.00
CV	50.00	1.92	6.51	1.37	35.28	1.81
RD	0.33	0.83	0.21	0.77	0.43	0.87
OM	0.03	0.55	0.01	0.46	0.01	0.49
B	0.00	0.27	0.00	0.27	0.00	0.23
Total = δ		**7.75 = 1sδ**		**8.62= 2sδ**		**12,14 = 3sδ**

This defuzzification stage produces precise, clear-cut information. The transformation of fuzzy information into specific information is called defuzzification [29]. In short, defuzzification is the transition from the "blurred world" to the "real world" [28]. Defuzzification can use a threshold defined subjectively or objectively by a fuzzy value [30].

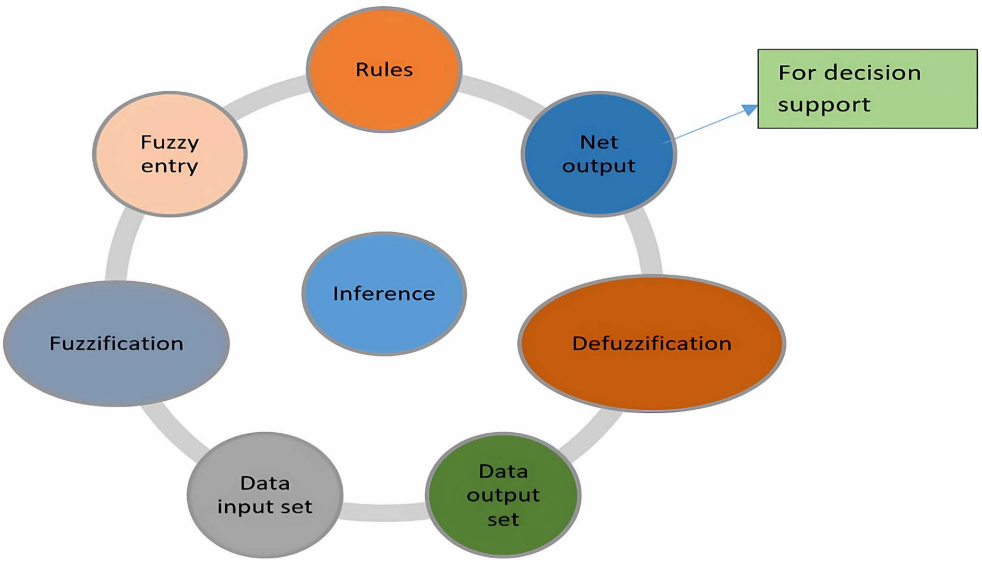

Figure 9. Fuzzy logic system [31].

Figure 9 shows the virtual organisation of the fuzzy logic system, which starts with the input data from the universe (fuzzification or blurring), lays down rules using a set of codes for perception, control, monitoring, processing and analysis (inference rules) and ends with an understanding of the data universe (defuzzification or defuzzing). It is, therefore, the process of decomposing a data input into an output using fuzzy inference rules [31]. The literature shows the existence of triangular, trapezoidal and Gaussian membership functions. With this in mind, we have taken the triangular membership function determined by Figure 9.

$$\delta_{\text{facteur}} = \sum_{1}^{n} \alpha_{\text{facteur}} \tag{7}$$

In step 3, we use technique 5, where each factor occurrence is normalised to unity; this involves dividing the occurrence of the factor by the sum of the occurrences of all the factors (Equation (7)).

$$\theta_{\text{facteur}} = \frac{\alpha_{\text{facteur}}}{\delta_{\text{facteur}}} \tag{8}$$

θ_{facteur} corresponds to the perception of a normalised factor divided by the sum of the perceptions of the normalised factors

$$\lambda_{\text{facteur}} = \frac{\sum_{1}^{n} (\theta_{\text{facteur}})}{n} \tag{9}$$

λ_{facteur} the perception of a normalised factor divided by the sum of the perceptions of the normalised factors and the whole divided by the number of factors.

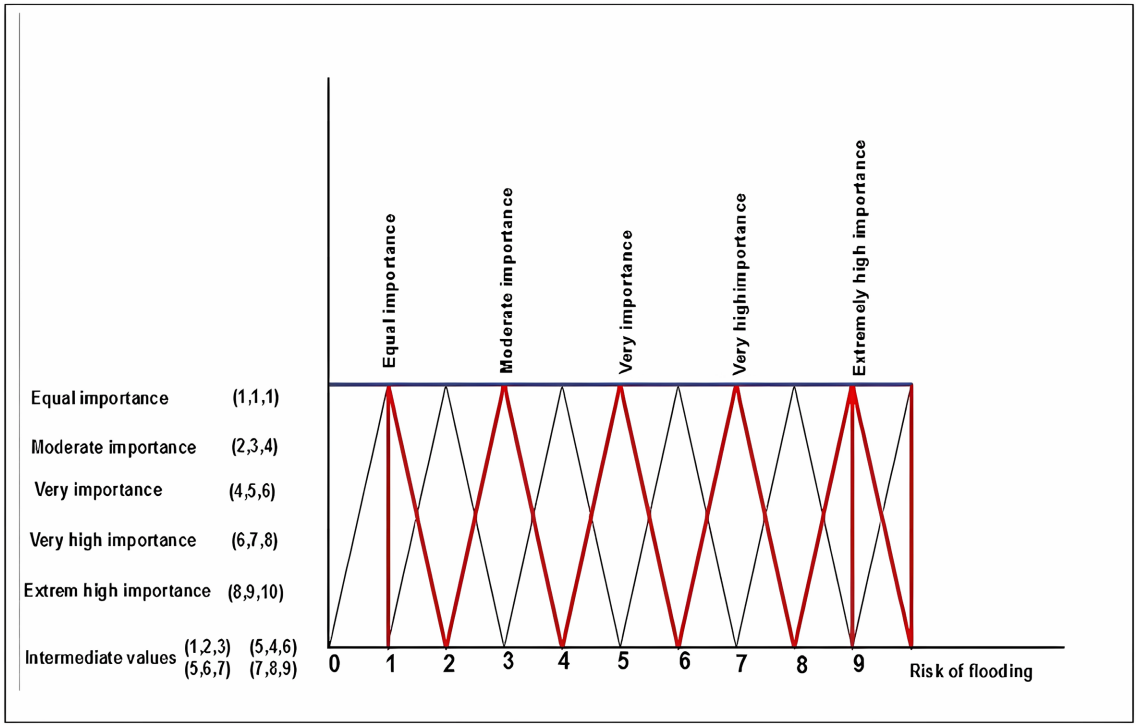

Figure 10. Fuzzy interpretation scale [31].

Table 10. Weighted defuzzification matrix of perceptions of ORSEC Plan members for the year 2022 according to the AHPF model.

Factor	$\theta_{facteur}$	$\theta_{facteur}$	$\theta_{facteur}$	$\theta_{facteur}$ in % of	$\Phi_{facteur}$ in % of
P	0.33	0.42	0.47	20	**41**
TSP	0.23	0.25	0.25	12	**24**
CV	0.15	0.16	0.15	8	**15**
RD	0.13	0.09	0.08	5	**10**
OM	0.1	0.05	0.04	3	**7**
B	0.06	0.03	0.02	2	**3**
Total	**1**	**1**	**1**	**50**	**100**

Table 11. Weighted defuzzification matrix of the perceptions of people affected by flooding for the year 2022 according to the AHPF model.

Factor	$\theta_{facteur}$	$\theta_{facteur}$	$\theta_{facteur}$	$\theta_{facteur}$ in % of	$\Phi_{facteur}$ in % of
P	0.32	0.43	0.47	20	**40**
TSP	0.22	0.24	0.25	12	**24**
CV	0.25	0.16	0.15	9	**19**
RD	0.11	0.09	0.07	4	**9**
OM	0.07	0.05	0.04	3	**5**
B	0.03	0.03	0.02	1	**3**
Total	1.00	1.00	1.00	50	**100**

$$\Phi_{\text{facteur}} = \frac{\lambda_{\text{facteur}}}{\sum_1^n (\theta_{\text{facteur}})} \quad (10)$$

Φ_{facteur} corresponds to the fuzzy weighting of a factor.

In step 4, we determine the net flood risk index (NFRI), which involves the following techniques.

In technique 6, we determine the Global Factor Vulnerability Index (GFVI) according to the following relationship:

$$\text{GFVI} = \sum \text{CP}_{\text{facteur}} \quad (11)$$

CP_{facte} is the factor weighting criterion.

In technique 7, we calculate the NFRI, which is the product of the rainfall hazard and the overall factor vulnerability index (IGVF). To do this, we apply Equation (12) below:

$$\text{IRI} = \text{Hazard}_{\text{rainfall}} * \text{GFVI} \quad (12)$$

The rainfall hazard is uniform across the study area. The spatial uniformity of the rainfall hazard means that its value is a constant and uniformly influences the NFRI over the entire study area. Consequently, if Aléapluviometry is equal to 1, the NFRI is equal to the IGVF.

$$\text{NFRI} = \text{GFVI} \quad (13)$$

5. Results and Discussion

Our study area covers 88.24 km² and lies between the 550 mm and 600 mm rainfall isohyets. The particularity of the study area lies in its size (less than 100 km²), the absence of rivers, lakes and streams and the fairly even spatial distribution of rainfall. To this end, we have shown that it is possible to model the risk of flooding without taking active factors into account and to focus on passive factors.

This particularity made it possible to analyse the degree of influence of vegetation cover and slopes in the occurrence of floods. Our surveys of ORSEC Plan members showed that, out of a total of 47 managers, 16.7% of fire brigades were aware of the very strong influence of vegetation cover on flooding. The same rate was observed among land registry, environment, surveyor and municipality managers. As for the perception of strong influence, 42.9% came from the fire brigade, 7.1% from the Prefect, 7.1% from the land registry, 7.1% from the sanitation department and 7.1% from the hydraulics department. In sum, we note that 13% of the managers surveyed said that vegetation had a very strong influence on flooding, compared with 30% for a strong influence and 57% for an average influence. This shows that the degree of influence of vegetation cover in the occurrence of floods is significant. The perceptions of the people affected by the floods show a trend towards very high and high vulnerability of the slopes to the risk of flooding. The surveys showed that 19% and 33% of neighbourhood representatives respectively said that the slopes were very vulnerable and highly vulnerable to flooding, compared with 48% who said they were moderately vulnerable. Religious guides said that 39% of slopes were very vulnerable to flooding and 39% were highly vul-

nerable, compared with 21% who said that slopes were moderately vulnerable. The same trend can be observed among members of grassroots community organisations, sports and cultural associations and women's groups. This perception analysis confirms that slopes play an important role in the occurrence of flood risk in the study area.

Our work has also shown that it is possible to model flood risk by taking into account endogenous knowledge (lessons learnt from the experience of stakeholders). Ultimately, our work has shown, unlike the authors [21] [23] [25] [31] who have focused on scientific techniques to predict the risk of flooding, that it is possible to combine endogenous knowledge, matrix calculations and geomatics to determine the mapping of the flood hazard using the flood risk index. Moreover, the results of the AHPF (Table 10 and Table 11) made it possible to determine the Net Flood Risk Index (NFRI) of the members of the ORSEC Plan and the people affected by the floods according to the following relationships:

$$\mathrm{NFRI}_{\mathrm{ORSEC2022}} = 0.41\mathrm{P} + 0.24\mathrm{TSP} + 0.15\mathrm{CV} + 0.10\mathrm{RD} + 0.07\mathrm{OM} + 0.03\mathrm{B} \quad (14)$$

$$\mathrm{NFRI}_{\mathrm{PERS2022}} = 0.40\mathrm{P} + 0.24\mathrm{TSP} + 0.19\mathrm{CV} + 0.9\mathrm{RD} + 0.05\mathrm{OM} + 0.03\mathrm{B} \quad (15)$$

These two NFRIs are used in the ArcGIS Weighted Overlay tab to automatically generate the flood hazard map.

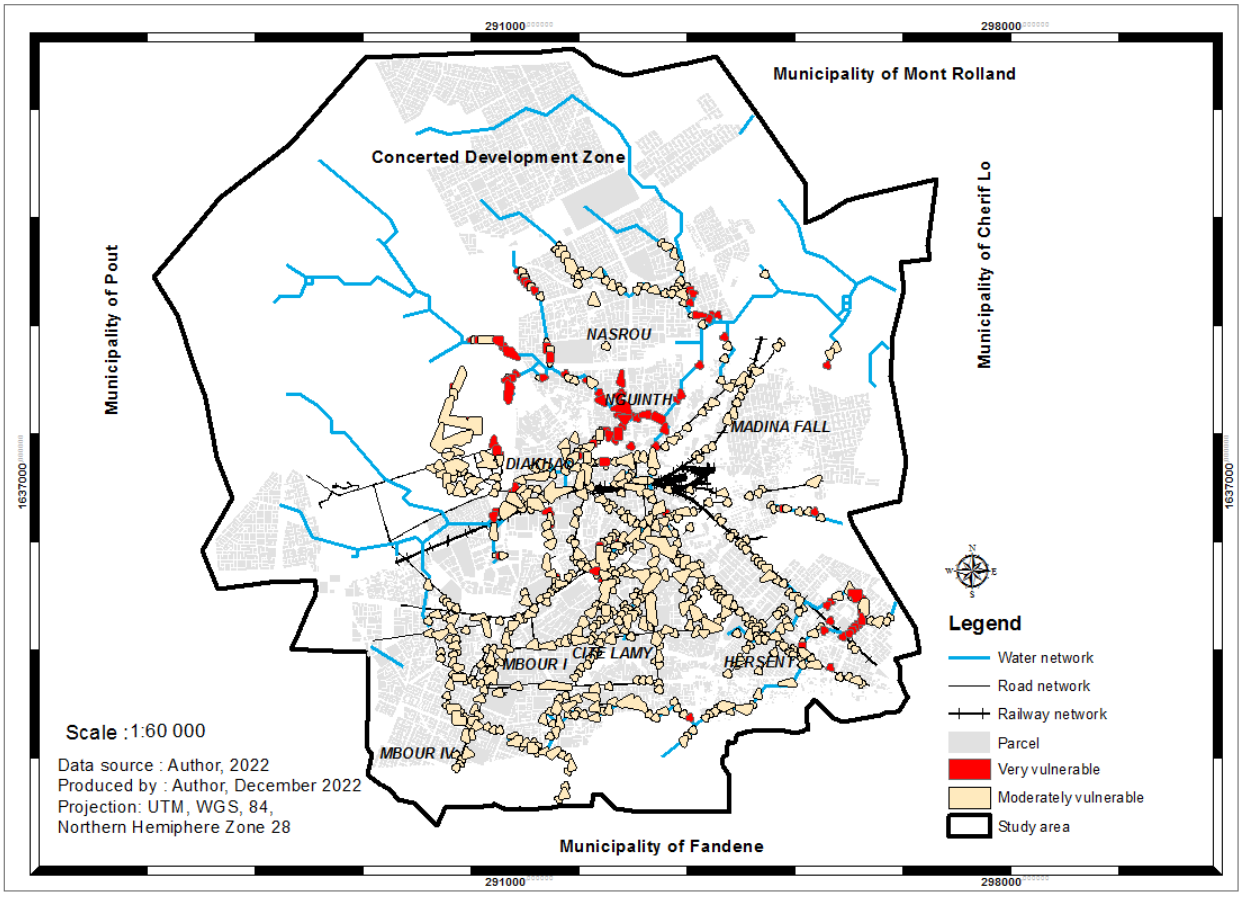

Figure 11. Flood hazard map based on the NFRI index of ORSEC plan members NFRI index.

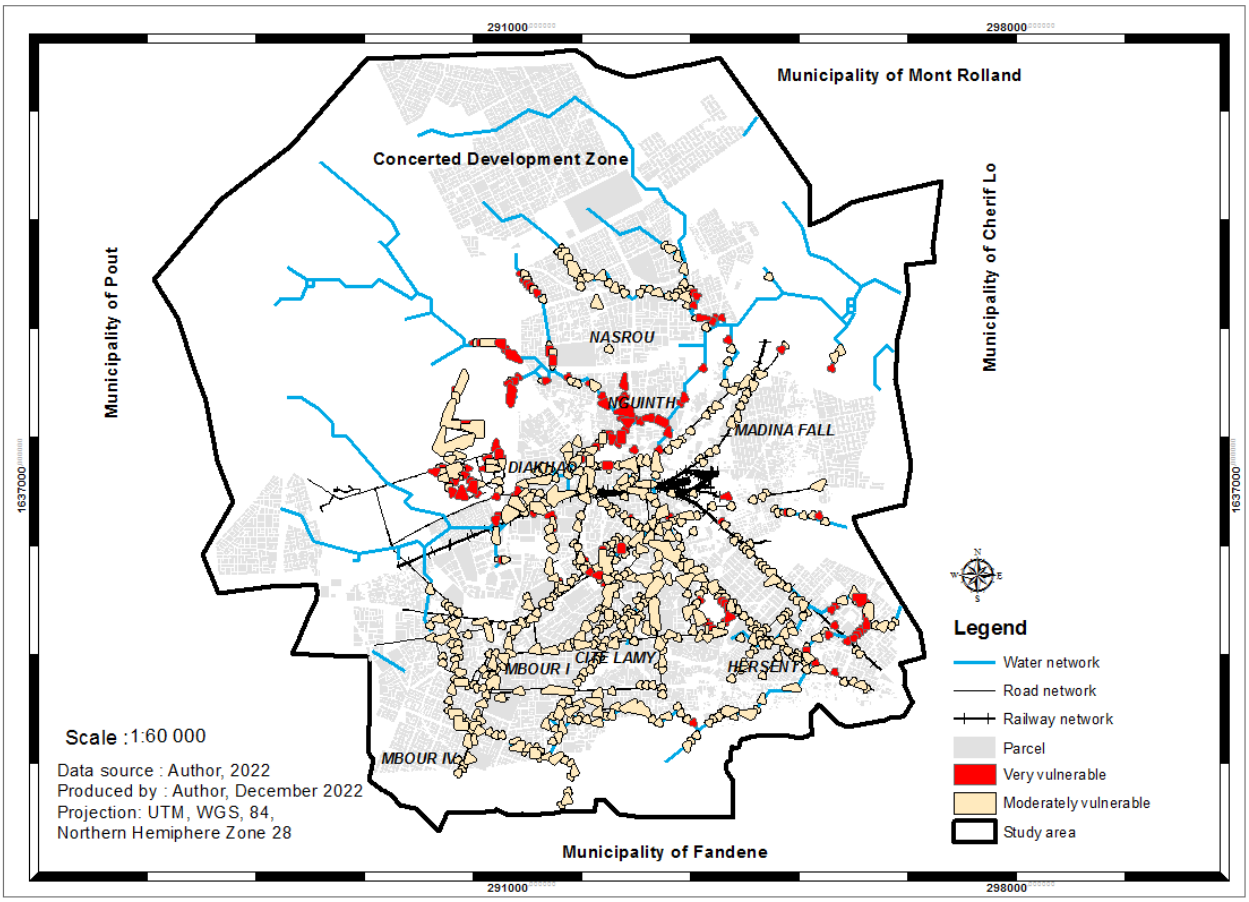

Figure 12. Flood hazard map based on the NFRI index of people affected by flooding for the year 2022.

Figure 11 and Figure 12 show the spatial distribution of the flood hazard in the study area, with the contribution of physical factors (slopes, soil type and vegetation cover) dominating over man-made factors (various networks, household waste and buildings). This means that physical factors have a much greater influence on the occurrence of flooding than man-made factors.

The cartographic analysis also enables us to appreciate, according to the AHPF model, the perception of the members of the ORSEC Plan (Figure 9), that out of a total of 1417 properties affected by very high vulnerability to flooding, 62.7% represent inhabited houses compared with 8.1% for infrastructures, 4.2% for houses under construction, 15.7% for plots of bare land and the remainder constituting other types of land occupation. Our calculations enabled us to determine the overall vulnerability rate for the study area, which is equal to the total vulnerable surface area (8.91 km^2) divided by the surface area of the study area (88.24 km^2). It is equal to 10%, giving a very high vulnerability rate of 1.4% compared with a medium vulnerability rate of 8.7%. Figure 10 not only confirms the flood hazard map according to the NFRI index of the perceptions of the members of the ORSEC plan, but also allows us to note a very high vulnerability to flooding in certain areas. In fact, this characteristic is present in all neighbourhoods except those located further west and north-west, where the highest areas are found.

6. Conclusion and outlook

In this study, we moved from the hierarchical process analysis (HPA) model to the fuzzy hierarchical process analysis (FHPA) model by determining the consistency indices and consistency ratios of the HPA, which are equal to 5%. This phase shows that the consistency of the data collected from the members of the ORSEC plan and the people affected has followed an acceptable approach. To this end, we developed the Hierarchical Fuzzy Process Analysis, which produced the Net Flood Risk Index (NFRI) based on stakeholders' perceptions. With the help of ArcGIS software, this index was used to automatically generate a flood hazard map for the area, where the contribution of physical factors predominates over man-made factors. This map revealed a very high vulnerability rate of 1.4%, affecting 1,417 properties, compared with an average vulnerability rate of 8.7%.

In light of all that has been said above, we propose, as part of the prevention and strengthening of the resilience of areas exposed to the risk of flooding, the implementation of an early warning system for the prevention and management of floods. This system would make it possible to prevent, prepare for and give early warning of natural disasters, particularly floods, using hierarchical Fuzzy Process Analysis. It could also assess physical damage and injuries and strengthen the resilience of high-risk areas. The system could be placed at the heart of a sub-regional and national observatory in which climatologists, forecasters and researchers will have to work in synergy to better manage natural disasters, particularly floods.

Acknowledgements

I would like to thank my parents for all their efforts on my behalf. This work was carried out within the University's Sustainable Development and Society Doctoral School de Thies (ED2DS) of the University Iba Der THIAM de Thies under the direction of Professor Mapathé NDIAYE. Throughout his years of research, he demonstrated pragmatism, rigour in his supervision and intellectual generosity so that this work could serve as a reference model. His perseverance and acute sense of duty have given me the confidence to rise to the challenges of research. I would also like to thank all the professors and Dr Issa NDOYE, who supported me at every stage of my research. To Professors Makhaly BA and Diogoye DIOUF of the Iba Der THIAM University in Thiès, thank you for your support and for continuing my research work. I would like to express my thanks to the Association of Land Registry Officers of Senegal.

Conflicts of Interest

The authors declare no conflicts of interest regarding the publication of this paper.

References

[1] Randriamparany, M.R.J.M.A. (2017) Rapid Mapping and Assessment of Flood Damage with Free Data and Open Source Software: The Case of the Sambirano Floodplain,

Madagascar. *Afrique Science*, **2**, 24-31.

[2] DMSG (2001) The Use of Earth Observing Satellites for Hazard Support: Assessments & Senarious. Committee on Earth Observation Disaster Management Support Group, Final Report, NOAA, USA: Dept. Commerce.

[3] Merz, B., Kreibich, H., Schwarze, R. and Thieken, A. (2010) Valuation of Economic Damages Caused by Floods. *Natural Hazards and Earth System Sciences*, **8**, 1697-1724.

[4] Bertoni, J.C. (2006) Urban Flooding in Latin America: Reflections on the Role of Risk Factors. *Frontiers in Flood Research*, **305**, 1123-1141.

[5] Niculescu, S., & Lardeux, C. (2007) Gestion durable des zones inondables dans le Delta du Danube (Roumanie). *Proceedings of the JSIRAUF*, Hanoi, 6-9 November 2007.

[6] OCHA (2009) West Africa: OCHA Newsletter. OCHA.

[7] Wallez, L. (2010) Flooding in West African CITIES: DIAGNOSIS and Elements for Strengthening Adaptation Capacities in Greater Cotonou. Master's Thesis, University of Cotonou.

[8] EM-DAT (2020) International Database on Natural Disasters.

[9] Sy, B., Frischknecht, C., Dao, H., Consuegra, D. and Giuliani, G. (2019) Reconstituting Past Flood Events: The Contribution of Citizen Science. *Hydrology and Earth System*, **24**, 61-74.

[10] Saaty, T. (1980) The Analytic Hierarchy Process (AHP) for Decision Making. *Kobe*, **1**, 69.

[11] Feizizadeh, B., Blaschke, T., & Nazmfar, H. (2014) GIS-Based Ordered Weighted Averaging and Dempster-Shafer Methods for Landslide Susceptibility Mapping in the Urmia Lake Basin, Iran. *International Journal of Digital Earth*, **7**, 688-708.

[12] Vahidnia, M.H., Alesheikh, A.A. and Alimohammadi, A. (2009) Hospital Site Selection Using Fuzzy AHP and Its Derivatives. *Journal of Environmental Management*, **90**, 3048-3056. https://doi.org/10.1016/j.jenvman.2009.04.010

[13] Naaz, S., Alam, A. and Biswas, R. (2011) Effect of Different Defuzzification Methods in a Fuzzy Based Load Balancing Application. *International Journal of Computer Science Issues*, **8**, 261-267.

[14] Weistroffer, H.R., Smith, C.H. and Narula, S.C. (2005) Multiple Criteria Decision Support Software. In: Weistroffer, H.R., Smith, C.H. and Narula, S.C., Eds., *Multiple Criteria Decision Analysis: State of the Art Surveys*, Springer, 989-1009. https://doi.org/10.1007/b100605

[15] Greco, S., Mousseau, V. and Słowiński, R. (2009) The Possible and the Necessary for Multiple Criteria Group Decision. In: Rossi, F. and Tsoukias, A., Eds., *Algorithmic Decision Theory. ADT* 2009, Springer, 203-214.

[16] Ramos, A., Cunha, L. and Cunha, P.P. (2014) Application of the Hierarchical Multicriteria Analysis Method to the Study of Landslides in the Coastal Region of Central Portugal: *Figueira da Foz-Nazaré. Geo-Eco-Trop*, **38**, 33-44.

[17] Cherif, B.M. (2014) Les méthodes multi-critères pour analyser les aptitudes des terres agricoles: Le cas du blé tendre en Languedoc-Rousillon analysé avec la méthode AHP. Université Paul Valéry de Montpellier, 61 p.

[18] Rakotoarivelo, J.B. (2018) Multi-Criteria Decision Support for Risk Management in the Financial Domain. Université Paul Sabatier.

[19] Blaschke, F.B.E. (2012) Comparison of GIS-Multicriteria Decision Analysis for Land-

slides, Sensitivity Mapping for Lake Urmia Basin, Iran. Center for Remote Sensing and GIS, University of Tabriz.

[20] Saaty, T.L. (1991) Some Mathematical Concepts of the Analytic Hierarchy Process. *Behaviormetrika*, **18**, 1-9. https://doi.org/10.2333/bhmk.18.29_1

[21] Belloula, M., Dridi, H. and Kalla, M. (2020) Spatialization of Water Erosion Using Analytic Hierarchy Process (AHP) Method in the High Valley of the Medjerda, Eastern Algeria. *Journal of Water and Land Development*, https://doi.org/10.24425/jwld.2019.127041

[22] Saaty, R.W. (1987) The Analytic Hierarchy Process: What It Is and How It Is Used. *Mathematical Modelling*, **9**, 161-176. https://doi.org/10.1016/0270-0255(87)90473-8

[23] Feizizadeh, B., *et al.* (2013) A GIS-Based Spatially Explicit Sensitivity and Uncertainty Analysis Approach for Decision Analysis. *Computers & Geosciences*, **64**, 81-95. https://doi.org/10.1016/j.cageo.2013.11.009

[24] Guitouni, A. (2016) The Engineering of the Choice of a Multicriteria Aggregation Procedure. Ph.D. Thesis, Laval University.

[25] Med, A. and Zine, A. (2019) Apport des SIG dans l'étude de la qualité des eaux souterraines par la méthode d'analyse hiérarchique des Procédés (AHP) dans la région Nord-ouest d'Elouad (Algérie), Northwest region of Elouad (Algeria). Echahid Hamma Lakhdar El oued University, Faculty of Technology.

[26] Lamachere, D. (1996) Hydrologie et modélisation à base de règles floues: Calcul du coefficient de ruissellement décennal. ORSTROM.

[27] Tuyisenge, L. (2019) Collecte des données Véhicule/Environnement et remontée avec réseau Cellulaire et réseau Véhiculaire. Thèse de doctorat, Université de Reims Champagne-Ardenne.

[28] Chevrie, F. and Guély, F. (1998) La logique floue. Cahier technique 191. Edition Schneider, Electric, Collection technique, 1-28.

[29] Dernoncourt, F. and Sander, E. (2011) La Logique Floue: Entre raisonnement humain et intelligence artificielle. Mémoire de master, 56 p.

[30] Sicat, R.S. (2004) Fuzzy Modelling of Farmers' Knowledge for Land Suitability Classification. National Economic and Development Authority (NEDA).

[31] Wang, C.-N., *et al.* (2021) Un modèle de sélection d'un fournisseur de four à biomasse basé sur des facteurs qualitatifs et quantitatifs. Article scientifique, publié sur la revue Tech Science Press. Département d'ingénierie et de gestion industrielles, Université nationale des sciences et technologies de Kaohsiung, 80778.